Chemical Engineering Journal 532 (2026) 174526

Contents lists available at ScienceDirect

Chemical Engineering Journal

journal homepage: www.elsevier.com/locate/cej

Hydrothermal carbonization of bioplastics and plastics: a promising approach for handling mixed waste

Filippo Marchelli [a,b], Claudio Gioia [c], Sara Lombini [a], Gianni Andreottola [a], Luca Fiori [a,d,*]

[a] Department of Civil, Environmental and Mechanical Engineering, University of Trento, Via Mesiano 77, 38123, Trento, Italy
[b] Department of Civil, Chemical and Environmental Engineering, University of Genova, Via all'Opera Pia 15a, 16145, Genova, Italy
[c] Department of Physics, University of Trento, Via Sommarive 14, 38123, Trento, Italy
[d] Center Agriculture, Food, Environment, University of Trento, Via Edmund Mach 1, 38098, San Michele all'Adige, Italy

ARTICLE INFO

Keywords:
Lactic acid
Thermal hydrolysis
Mater-Bi
Compostable plastics
Postconsumer plastics

ABSTRACT

The growing production of biodegradable plastics and the frequent mismanagement of their end-of-life often lead to mixed waste streams containing both bioplastics and conventional plastics, which create challenges for mechanical recycling. Hydrothermal carbonization (HTC) has been proposed as a pre-treatment enabling chemical recycling or anaerobic digestion of bioplastics, but its application to bioplastic-plastic mixtures has not been investigated. In this study, seven plastics—two compostable bioplastics items (based on PLA, PBAT, and starch) and five conventional plastics (PET, HDPE, LDPE, PS, PP)—were subjected to HTC, individually and in mixtures. Results show that PLA and starch hydrolyse readily at 180 °C, PBAT requires at least 200 °C, and PET hydrolyses to monomers at 220 °C, while the three polyolefins and PS remain unaltered even at 250 °C. Processing mixtures shows no major effects on yields and compositions, but presents a notable practical advantage: bioplastics disintegrate and hydrolyse, dispersing or dissolving in the liquid phase, while conventional plastics coalesce into a compact solid block atop the liquid. This enables effective qualitative separation of bioplastics and plastics, allowing the former to be directed to anaerobic digestion or chemical valorisation and the latter to thermochemical processes.

1. Introduction

The management of mixed plastic waste remains a significant challenge for modern treatment systems. In principle, most waste plastics should be morphed into new products through mechanical recycling, but in practice numerous obstacles persist [1], and only 8.9% of global plastic production in 2022 originated from mechanically recycled feedstock [2,3]. Mechanical recycling relies on a good separate collection of waste plastic items, followed by sorting at recycling facilities according to polymer type. Several obstacles hinder this process: some are related to citizens' behaviour, such as discarding non-plastic items with plastics and vice versa; others concern the properties of the items themselves, including the presence of additives, multilayer structures, or small objects that are difficult to sort [4]. In recent years, the growing presence of biodegradable plastics has also further complicated plastics recycling.

Biodegradable plastics are a class of materials whose production is indeed undergoing a strong and steady surge [5]. In common usage (and in this article as well), they are often referred to as "bioplastics", although the term is often employed also for biomass-based plastics that are chemically identical to traditional fossil-based plastics. Commercial bioplastic items are certified to be compostable, and hence they are often advised to be sent to the plants that treat the organic fraction of municipal solid waste (OFMSW). They may cause some problems even within this treatment chain, often due to their long degradation times or unsuitability for anaerobic digestion (often employed before composting) [6], but this aspect is outside the scope of this work. Oftentimes, bioplastics may not even enter composting treatment chains, but end up in different destinations:

- Reject fraction of OFMSW treatment plants. These plants typically use size-based mechanical pre-treatments to remove large objects that cannot degrade within suitable time frames [7,8]. These may include branches, bones, plastic objects, inert materials, etc. Due to their large size and stiffness, bioplastic items are often also caught by this pre-treatment.

* Corresponding author at: Department of Civil, Environmental and Mechanical Engineering, University of Trento, Via Mesiano 77, 38123, Trento, Italy.
E-mail address: luca.fiori@unitn.it (L. Fiori).

https://doi.org/10.1016/j.cej.2026.174526
Received 31 October 2025; Received in revised form 28 January 2026; Accepted 22 February 2026
Available online 24 February 2026

- Unrecyclable mixed plastic waste. Consumers' confusion [9–12] may lead to bioplastics being discarded with conventional plastics, even when legislation prohibits this. As already described, mechanical recycling facilities sort waste items based on their constituent polymer. In principle, bioplastics are suitable for mechanical recycling, and some researchers even argue that this should be the first choice for them [13]. However, plants are often not equipped to deal with them [14], usually because they only represent a small fraction of processed waste. Consequently, they are collected alongside other items that, for various reasons, are unsuitable for mechanical recycling [15,16]. Bioplastics and plastics can also be found together in mixed polymer items, such as multilayer films employed in agriculture [17], which are unsuitable for mechanical recycling.
- Other mixed waste streams. Where separate collection is absent, inefficient, or guided by unclear regulations, bioplastics may end up in residual waste.
- The environment. Bioplastics may end up in the environment (fields, oceans, etc.) for different unwanted reasons. In these conditions, they tend to degrade faster than fossil-based plastics, but may still remain unaltered for many years, posing threats to living organisms [18,19]. Mixed debris can be intercepted by different technologies and removed from the environment [20], and then appropriately disposed of.

To sum up, waste bioplastics frequently occur mixed with conventional plastics. While other contaminants can often be removed via magnetic or gravimetric separation, separating bioplastics and plastics is more challenging, especially when they are fragmented or closely intertwined. Mixed plastics-bioplastics can be processed together via thermochemical routes such as pyrolysis or gasification or other more advanced techniques [21], enabling chemical recycling. Although this is feasible in principle and has been demonstrated at the lab scale for plastics [22,23], industrial implementation is hindered by the problematic rheological behaviour of molten plastics, high energy demands, and contamination with organic residues or inorganic elements (e.g., chlorine, bromine), often requiring pre-washing or drying. A method capable of selectively separating bioplastics from plastics would therefore be valuable: it could reduce the fraction requiring thermochemical treatment and, in the case of pyrolysis, improve product quality by lowering feedstock oxygen content. Hydrothermal processes offer a promising approach, as they are known to degrade bioplastics while leaving conventional plastics largely intact.

Low-temperature hydrothermal processes (or also “hydrothermal treatments”) comprise thermal hydrolysis (performed at 140–180 °C) and hydrothermal carbonization (HTC, performed at 180–250 °C). These processes take place in pressurised units, with high-temperature liquid water acting as a catalyst that facilitates various degradation reactions. They are typically applied to wet biomass residues to make them more suitable for anaerobic digestion [24] or to synthesise a sterilised solid product (called hydrochar) with enhanced carbon concentration and dewaterability [25,26]. In the last 5 years, various researchers have proven that these processes can also be applied to bioplastics, achieving complete hydrolysis at moderate temperatures [8]. The resulting liquid product is often very rich in bioplastics monomers or other organic acids, allowing a more productive anaerobic digestion or possibly chemical recycling. Most research has focused on poly(lactic acid) (PLA), often treated at $\leq$150 °C, sometimes with added bases to accelerate hydrolysis [27–31]. Without alkaline additives, 180 °C seems instead the minimum treatment temperature that can guarantee the full hydrolysis of PLA and other bioplastics [32], coinciding with the lower HTC temperature limit. While PLA is the major biodegradable polymer being produced at the moment and in the foreseeable future, starch blends also play a major role [5], especially in selected countries where they are employed to produce disposable shopping bags [33].

Hydrothermal treatment of conventional plastics has been less explored. A very broad overview of the behaviour of plastics in thermal conditions was provided by Yang et al. [34], while other reviews were more focused on hydrothermal processes [35]. Nonetheless, the overall number of studies dealing with plastics in HTC is quite limited, especially with products tested separately. Most plastics are considered chemically stable under HTC conditions, though they may become denser and transfer inorganic contaminants to the liquid phase. For example, Farru et al. [36] reported that HTC of polypropylene (PP) and polyester surgical masks produced a compact solid with a 75% volume reduction but unchanged composition. Iñiguez et al. [37] applied HTC to marine plastic debris, observing enhanced fuel properties, dechlorination and debromination. Lin et al. [38] employed various types of urban waste, confirming that polyethylene (PE) and PP are not affected by the process apart for their physical appearance, which becomes more compact. Similarly, Zhao et al. [39] reported no chemical change for high-impact polystyrene (PS), acrylonitrile butadiene styrene (ABS), and PP at 250 °C, though polyamides and polycarbonates behaved differently. Mixed biomass-plastic HTC studies have shown synergies in fuel properties [40–42], while a very interesting point of the work by Farghali et al. [43] was the use of HTC to solubilise the food waste attached to plastic bags prior to anaerobic digestion.

The two general-use polymers that seem more affected by the process are poly(ethylene terephthalate) (PET) and poly(vinyl chloride) (PVC). PET, as a polyester, can hydrolyse in HTC conditions, yielding its constitutive monomers [44]. Complete hydrolysis typically occurs between 220 and 250 °C, depending on factors such as particle size, residence time, and reactor design, but is also feasible at lower temperatures with longer residence times [45]. Notably, terephthalic acid formed during PET hydrolysis acts as a self-catalyst, allowing even higher efficiency by recycling the process water to the reactor [46]. For PVC, HTC can transfer chlorine to the liquid phase, yielding a chlorine-free solid appropriate for dioxins-free combustion. Poerschmann et al. [47] were among the first to test PVC in HTC, indicating 235 °C as the minimum temperature for complete dechlorination. PVC has also been tested in combination with biomass, with reported benefits in terms of dechlorination and energy densification [48–53].

Despite these advances, important gaps remain: several common plastics have never been individually tested in HTC conditions, and the co-processing of bioplastics and plastics under HTC has not been previously reported. This work addresses both gaps through a systematic investigation of the HTC of bioplastics and conventional plastics, alone and in mixtures, confirming that the process can hydrolyse bioplastics while compacting plastics, enabling their physical separation. This separation, never addressed before in the literature, is very promising for the application of this process to the various aforementioned mixtures of bioplastics and plastics, potentially allowing the two product classes to be valorised through ad hoc pathways. The study examines real commercial items—two bioplastics (disposable PLA spoons and Mater-Bi® shopping bags) and five conventional plastics (PET, HDPE, LDPE, PS, and PP)—subjected to four treatment temperatures across the HTC range.

2. Materials and methods

2.1. Tested samples

The experiments focused on two bioplastic items and five conventional plastic items. All of them were commercial products purchased at local shops.

The two bioplastic families, certified as compostable according to UNI EN 13432/02, were:

- BPBAGS: Two compostable Mater-Bi® bioplastic bags used in Italian supermarkets (shopping bags and produce bags). While the producer company does not disclose the composition of Mater-Bi® blends and several blends exist, Mater-Bi® is generally marketed as a mixture of starch, polyesters, and plasticisers.

- cPLA: Compostable spoons in crystallised poly(lactic acid), already tested at lower temperatures [32].

These two bioplastic families were specifically targeted since they account for approximately 62% of the total 2024 production of biodegradable plastics [54]. The five conventional petroleum-based plastics studied were:

- PET: Transparent blue sparkling water bottles in poly(ethylene terephthalate).
- HDPE: Caps of the above bottles, in high-density polyethylene.
- LDPE: Transparent bags in low-density polyethylene.
- PS: Transparent single-use forks in polystyrene.
- PP: Caps of yogurt jars in polypropylene.

We selected these materials due to their high market penetration for everyday objects. Conversely, we decided not to employ poly(vinyl chloride) (PVC): despite its large-scale production, it is mainly used for specialty applications such as tubes and cables, so it is less likely to amass in the mixtures described in the introduction. Moreover, as we have explained, its behaviour in HTC conditions is already well studied.

The reported materials were subjected to ash determination, elemental analysis, and Fourier-transform infrared spectroscopy (FTIR). Details on these techniques are provided in Section 2.3.

We also used corn starch (practical grade, Sigma-Aldrich) as a reference material.

2.2. HTC experiments

We performed the HTC experiments in a 50 mL unstirred lab-scale HTC reactor, already described in detail in previous publications [55]. We did not subject the bioplastics and plastics to any pre-treatment before feeding them to the reactor, apart from cutting them into roughly 2-cm pieces to facilitate their introduction into the reactor. The experiments were performed for each material singularly and for a mixture (noted as MIX). The mass composition of the MIX was the following:

- 25% each of BPBAGS and cPLA
- 10% each of PET, HDPE, LDPE, PS, and PP

All experiments were conducted at least in duplicate. We first filled the reactor with roughly 2.5 g of the tested sample and the amount of tap water needed to ensure a 0.10 mass ratio between the substrate and water (usually denoted as B/W, “biomass to water”). The only exception was LDPE, which was tested at a ratio of 0.05 because its low density made it difficult to fill the reactor with the necessary amount. The tested temperatures were 180, 200, 220, and 250 °C, and the residence time was always 1 h (calculated at the reaching of the set temperature). HDPE, LDPE, PS, and PP alone were only tested at 250 °C after verifying their lack of degradation in this condition. Temperatures lower than 180 °C were not tested because they cannot ensure bioplastics degradation [32], while temperatures higher than 250 °C would fall in the range of hydrothermal liquefaction, which is already known to be effective in degrading plastics, although requiring substantially more energy [56].

After filling the reactor with the samples and water, we closed it and flushed it three times with pressurised nitrogen to create an inert atmosphere and verify the lack of leakages. Then, we turned on the heating system, which relies on an electrical resistance and a thermocouple to create and maintain the desired thermal conditions. The reactor required roughly 15–25 min to reach the target temperature, depending on its value. The clocking of the 1 h process time was started once the thermocouple first recorded the set temperature, which remained stable for the entire time with only a maximum 5 °C overshot at the beginning. During the process, the pressure inside the reactor remained slightly above the saturation pressure of water at the corresponding temperature, confirming the absence of leakages. After 1 h at the set temperature had passed, we quickly cooled the reactor down by dipping it in cold water. Once its internal temperature was lower than 50 °C, we allowed the produced gas to flow into a transparent plastic column, filled with water and closed at the top, measuring its volume. The reactor was finally opened and its content vacuum filtered using a 0.45 μm quantitative filter membrane (in some cases, more than one membrane was necessary). In the cases in which a solid block of plastics was found at the top of the reactor, it was manually detached from the thermocouple and placed in the reactor for the drying phase. The reactor and the filter, both containing the separated solids, were dried overnight at 105 °C and then weighted together to assess the total quantity of solid resulting from the process. The solid was then stored at ambient temperature, while the liquid was stored in a fridge at 4 °C.

Solid yield (SY) was calculated as the percentage ratio between the dried solid mass and the initial mass of (bio)plastics. Gas yield (GY) was determined from the measured gas volume using the ideal gas law, assuming it consisted entirely of CO_2. This assumption is consistent with the HTC literature: the researchers that analyse the gas phase always report CO_2 to comprise at least 95% of it [57]. Since CO_2 has the highest molecular mass among common gas-phase compounds, this approach provides an upper boundary for the GY. Liquid yield (LY) was calculated as the 100's complement of SY and GY.

The solid products were subjected to the same analytical techniques as the starting products: ash determination, elemental analysis, and FTIR. The liquid product was instead checked for its pH, concentration of total organic carbon (TOC), and composition via ^{1}H nuclear magnetic resonance (NMR). More details are provided in the next sub-section.

2.3. Analytical techniques

The ash content of the initial bioplastics and plastics and of the solid HTC products was determined by placing a small amount of them in a muffle at 550 °C for 6 h, checking the weight before and after. Their elemental composition was assessed through a LECO 628 Elemental Analyser following ASTM D-5375, which yields the mass percentages of carbon (C), hydrogen (H), and nitrogen (N). The oxygen (O) mass percentage was determined as the 100's complement of C, H, N, and ash. The solids were also subjected to FTIR, employing an Agilent Cary 630 FTIR spectrometer. As the HTC of HDPE, LDPE, PS and PP and the MIX produced compact solid blocks of plastics, to perform the previous analyses they were crushed through an analytical mill (IKA® A11).

The pH values of the liquid products were measured through a ProfLine pH 3310 (WTW). The TOC concentration was obtained via a FORMACS HT-iTOC analyser (Skalar Analytical B.V., Netherlands) according to the ASTM D7573 standard.

NMR spectra (^{1}H NMR, ^{13}C NMR, and HSQC) were recorded on a Bruker Avance 400 MHz NMR spectrometer by using a 5 mm BBI probe with a 90° proton pulse length of 8 μs at a transmission power of 0 db. ^{1}H NMR quantifications were performed following a previously optimised procedure [58]. Samples were prepared by diluting 0.2 mL of HTC liquid with 0.4 mL of D_2O, which contained 0.05% *w*/w of 3-(trimethylsilyl) propionic-2,2,3,3-d_4 acid sodium salt (TSP). TSP served as both a reference standard ($\delta H = 0.00$ ppm) and a calibration standard (C(TSP) = 3.2 mM). The mass yields of compounds dissolved in the liquid phase were determined from NMR concentrations ($C_{i,liq}$), also considering the mass increase of the liquid phase due to the liquid yield. These values were then expressed as yields, i.e., ratios between the mass of each compound in the liquid phase ($m_{i,liq}$) and the initial mass of the treated sample (m_0). As explained in Ischia et al. [59], these yields can be calculated employing Eq. 1:

$$\frac{m_{i,liq}}{m_0} = \frac{C_{i,liq}}{\rho_{liq}}\left(\frac{1}{B/W} + LY\right) \quad (1)$$

Where ρ_{liq} is the density of the HTC liquid, assumed equal to 1000 kg/m^3. The yields are expressed in mg/g$_0$, where the subscript 0 denotes the initial treated sample. All the previous measurements were performed at least three times.

The accuracy of the performed measurements was assessed through a carbon balance, whose results are reported in the Supporting Information (Fig. S30). The analysis showed that the analytical techniques can correctly trace the fate of carbon in the HTC process: the average overestimation of the carbon in the products is 0.7%, it is above 15% only in two cases (cPLA treated at 180 and 200 °C) and is below −10% in only two cases (BPBAGS treated at 250 °C and PET treated at 220 °C).

3. Results and discussion

3.1. Compostable bioplastic bags

Novamont Mater-Bi® consists of a family of blends that combine starch and different polyesters, degradable under industrial composting conditions. In this work, we investigated the composition of Mater-Bi® used in compostable produce bags for grocery stores (noted as BPBAGS). Initially, two types of compostable bags were considered: supermarket shopping bags and produce bags. However, since the two materials presented similar composition (Fig. S1 and Fig. S2), only the produce bags were further tested in the HTC experiments.

Fig. 1 presents the FT-IR spectrum of BPBAGS. Comparison with previously reported spectra confirms that this material is mainly based on starch and poly(butylene adipate-*co*-terephthalate) (PBAT). Characteristic absorption peaks of PBAT are observed at 1714 cm^{-1} for the carbonyl (C=O) groups in ester linkages, at 1269 cm^{-1} for the C–O bonds in ester linkages, and a distinct peak at 729 cm^{-1} corresponding to adjacent methylene groups. The remaining peaks, primarily in the ranges of 3600–3000 cm^{-1} and 1200–950 cm^{-1}, are predominantly attributed to the starch component [60]. PBAT is the third most abundantly produced type of biodegradable plastic [54], with applications in multiple industrial sectors and frequent occurrence in blends with starch and PLA [61].

Further ^{1}H NMR, ^{13}C NMR, and HSQC analysis (Fig. 2, Fig. S3, Fig. S4), performed on the $CDCl_3$ soluble fraction of BPBAGS, demonstrated the presence of a mixture of polymeric structures, all contributing to the material formulation along with PBAT. Indeed, Fig. 2 confirms the presence of PBAT as the main component with the typical signals at 8.09 ppm (a) for the aromatic ring, at 4.40 (b) and 4.10 (f) ppm demonstrating the presence of a *co*-polymeric system with adipic acid, with its typical signal at 2.34 ppm (d). Furthermore, the signal (m) at 5.16 ppm is consistent with poly(lactic acid) (PLA), signal (e) at 3.56 may be referred to polyethylene glycol (PEG) units, while the singlet (h) at 2.62 ppm is consistent with the succinate unit and could be involved in compostable materials such as poly(butylene succinate) (PBS) or poly (butylene succinate adipate) (PBSA). It is worth mentioning that the formulation may involve additional components, additives, and plasticizers, which may further complicate the material composition. The ^{13}C NMR reported in Fig. S3 further confirms the presence of the aforementioned polymeric structures.

The HTC process was performed at different temperatures ranging from 180 to 250 °C. In all cases, BPBAGS underwent extensive degradation, yielding a mixture of partially hydrolysed products. Visually, solids obtained after filtration and drying are rather sticky and cohesive at lower temperatures, while they become darker and more powder-like after HTC at 220 and 250 °C. Table 1 summarises the yields and main properties of the products. As with other biogenic feedstocks, solid yield (SY) decreases with increasing temperature, accompanied by higher total organic carbon (TOC) concentrations and lower pH in the liquid phase, indicating enhanced solubilisation of organic matter. Unlike typical lignocellulosic materials, the C/H and C/O ratios of the solid did not increase with temperature: HTC does not concentrate carbon in the solid phase for BPBAGS, and the elemental composition remains similar to the starting material. Since PLA fully hydrolyses at ≥180 °C [32], the obtained solid product is likely ascribable to the starch and PBAT fractions. However, no work has ever been performed on the HTC of these two separately, and this is the first work reporting the HTC of a PBAT-containing material, so no comparison with the literature is possible.

Fig. 3 shows the FTIR of the solids resulting from the HTC experiments. A qualitative analysis evinces the substantial decrease of the signal related to starch (3280 cm^{-1} and 1200–950 cm^{-1}), with the concomitant appearance of multiple broad signals between 3120 and 2470 cm^{-1} related to the -CH bending of a variety of new architectures. A most relevant difference consists in the carbonyl signals at about 1700 cm^{-1} highlighted in the box in the central lower area of the figure: the change in the shape of the signal, along with the shift toward lower values, indicates the presence of different ester species and the

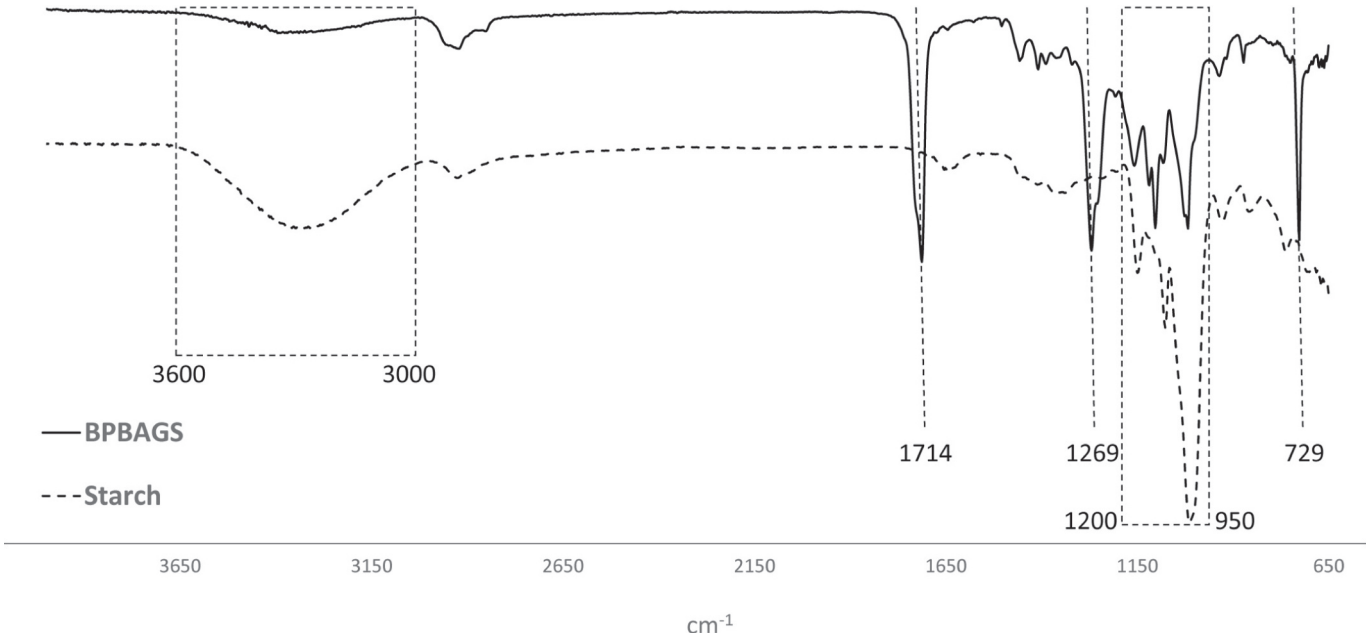

Fig. 1. FTIR spectra of BPBAGS and lab-grade corn starch.

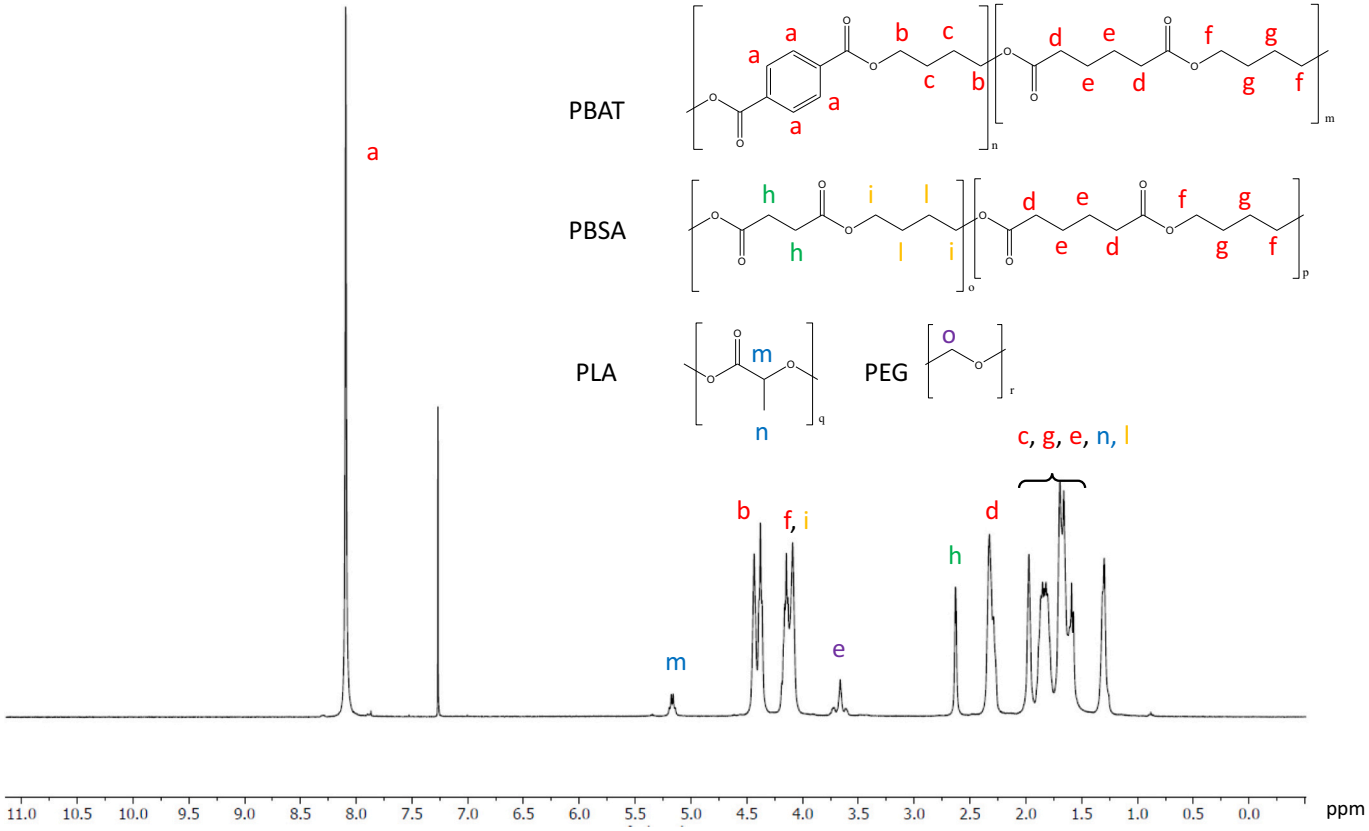

Fig. 2. ^{1}H NMR spectra of raw BPBAGS.

Table 1
Product yields and properties of the different phases from the HTC of BPBAGS.

HTC temp (°C)	Solid[a]				Liquid			Gas
	SY (%)	C (%)	H (%)	O (%)	LY (%)	TOC (g/L)	pH	GY (%)
Raw	–	55.7	7.6	36.6	–	–	–	–
180	68.6 ± 1.5	61.9	7.6	30.4	30.8 ± 2.4	16.2 ± 0.1	4.21	1.3 ± 0.9
200	65.0 ± 5.0	61.3	7.4	31.2	33.9 ± 5.8	15.3 ± 0.1	3.98	1.1 ± 0.8
220	46.4 ± 5.1	63.5	6.8	29.6	52.2 ± 6.2	25.3 ± 0.3	3.82	1.5 ± 1.2
250	34.5 ± 3.0	58.6	4.5	36.7	64.4 ± 3.5	24.5 ± 2.4	3.86	1.1 ± 0.5

[a] N and ash not indicated as they were null in all cases, standard deviations lower than 0.3%.

formation of carboxylic acids due to hydrolysis. This tendency is further confirmed by the appearance of the signals at 1420 and 928 cm^{-1}, consistent with carboxylic -OH bending along with the decrease of the signal at 1090 cm^{-1} related to the presence of methylene groups (-CH_2-).

Fig. 4 shows the results of the liquid phase ^{1}H NMR analysis (Figs. S5-S8), highlighting the noteworthy role that temperature plays in the degradation pattern. At 180 °C, starch and PLA are mainly degraded with the formation of amylose (75.5 mg/g_0), glucose (121.2 mg/g_0), and lactic acid (27.3 mg/g_0) (Fig. S5). Ethylene glycol, derived from PEG acid hydrolysis, can be detected in a range of 12.8 to 16.7 mg/g_0 at all the tested temperatures. At 200 °C, amylose becomes undetectable; however, the NMR can still detect glucose and 5-HMF as the main degradation products, along with a higher amount of lactic acid (Fig. S6). Adipic acid and butanediol appear as the main hydrolysis products of PBAT, becoming detectable at 200 °C and reaching their maximum at higher temperatures (220 °C for butanediol and 250 °C for adipic acid), while tetrahydrofuran (THF) at 220 and 250 °C most likely derives from the cyclisation of butanediol. At 220 °C, HMF and lactic acid can still be detected as residual products from starch and PLA, while the PBAT hydrolysis products become more abundant, with the appearance of phthalates (18.0 mg/g_0) (Fig. S7). At 250 °C, the highest amounts of the PBAT hydrolysis products can be detected, and while lactic acid reaches its maximum yield, none of the starch products are detectable anymore (Fig. S8). This suggests that they may undergo a repolymerisation (similarly to the products of cellulose acetate hydrolysis [59]), but the seemingly low fraction of starch in the starting material does not allow observing this effect in the SY, which decreases with temperature mainly due to the influence of PBAT getting further dissolved.

It is difficult to draw definitive conclusions on such a complex degradation pattern, but some considerations can be deduced. Indeed, 180 °C can be considered the best temperature for a pre-treatment of BPBAGS before biological processes, since the most abundant degradation products (amylose, glucose, and lactic acid) are naturally occurring molecules that usually pose no problems to microorganisms. The fact that HTC disintegrates BPBAGS already at this temperature also avoids the mechanical and hydraulic problems that these items face in anaerobic digestors. The products that form at higher HTC temperatures may still be acceptable for industrial composters, but are likely to inhibit anaerobic bacteria and possibly cause problems to the whole process, similarly to what happens with biomasses [24,62]. This is the case of phthalates, THF, and HMF, which have been repeatedly reported as toxic (more details on this aspect are reported in Section 3.6). At the same time, these compounds are all industrially relevant, so the process may be more interesting at higher temperatures if its purpose is to recover chemicals, provided that the bags are recovered with a sufficient level of purity.

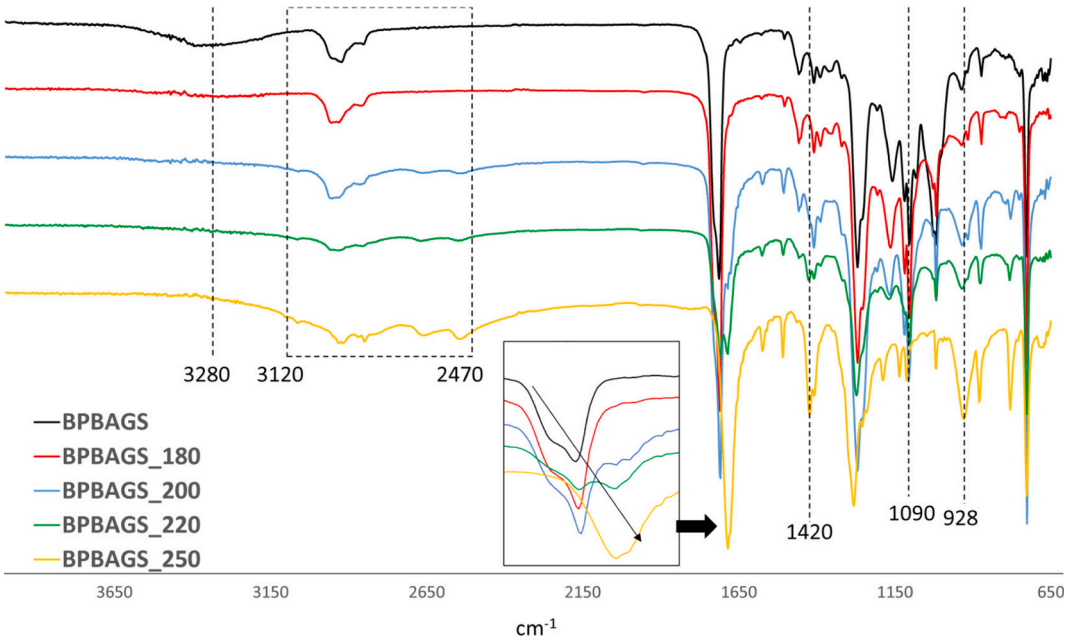

Fig. 3. FTIR spectra of BPBAGS and the solid fractions after the HTC process.

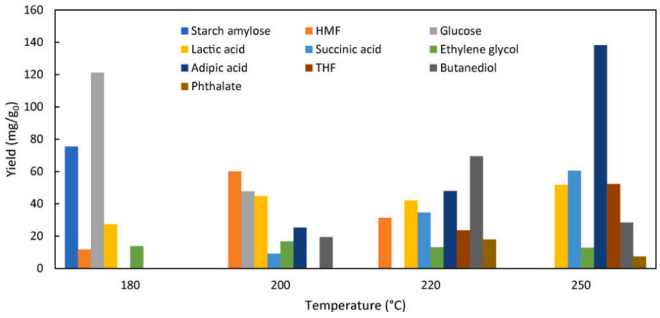

Fig. 4. Yields of products in the liquid phase from the HTC of BPBAGS; the values for starch amylose and phthalate were calculated employing the molecular masses of the amylose monomer and dimethyl phthalate, respectively. Refer to the nomenclature section for the acronyms.

3.2. Crystallised poly(lactic acid)

The HTC of PLA has already been investigated in our previous work [32] and by others at moderate temperatures [8]. Here, the study is extended to the higher temperature range of HTC: Table 2 shows the results.

A temperature of 180 °C is usually indicated as the minimum value to consistently hydrolyse PLA, which is confirmed for the cPLA employed in this study. Here, the SY remains close to 20% due to the ash content of the initial items: actually, the residual solid is nearly entirely comprised of ash. Increasing the HTC temperature up to 250 °C brings neither additional benefits nor negative effects relevant to downstream processing: in particular, we do not observe condensation of dissolved compounds into so-called secondary char [58], typically detected when dealing with lignocellulosic biomasses. The NMR analysis of the liquid phase (Figs. S9-S12) confirms these considerations: lactic acid is the only product detected in significant quantities, and its maximum yield is observed at 180 °C, very moderately decreasing at the higher tested temperatures. This might indicate that moderate repolymerisation may be taking place. At the same time, we do not observe the formation of any other significant pollutant, which lays the ground for a potential recovery of the lactic acid, or for its disposal through anaerobic digestion.

3.3. Poly(ethylene terephthalate)

The tests on PET confirmed the behaviour usually described in the literature (already summarised in the Introduction). Table 3 presents the yields and properties of the products obtained from the tests, while Fig. 5 shows the appearance of the recovered solids at different treatment temperatures. Visually, the PET pieces appear nearly unchanged after the test at 180 °C, apart from a slight curling and loss of transparency. Some disintegration starts happening at 200 °C, but the fragments are still detectable and recognisable. Conversely, at 220 and 250 °C, the solid product is a powder, completely different from the bottle pieces initially placed into the reactor.

Table 2
Product yields and properties of the different phases from the HTC of cPLA.

HTC temp (°C)	Solid[b]					Liquid				Gas
	SY (%)	C (%)	H (%)	O (%)	Ash (%)	LY (%)	TOC (g/L)	pH	Lactic acid yield (mg/g_0)	GY (%)
Raw[a]	–	41.2	5.2	34.1	19.5	–	–	–	–	–
180[a]	30.6 ± 2.2	4.8	1.4	8.5	85.3	68.7 ± 2.2	43.0 ± 0.7	3.32	872.6	0.8 ± 0.2
200[a]	29.2 ± 2.0	4.5	1.3	1.3	92.9	70.0 ± 1.8	44.7 ± 0.4	3.30	808.3	1.2 ± 0.8
220	29.1 ± 1.5	0.6	0.7	2.6	96.0	69.1 ± 1.4	36.2 ± 0.8	3.40	782.9	1.7 ± 0.3
250	25.8 ± 1.6	0.4	0.6	3.0	96.0	71.8 ± 0.3	36.5 ± 0.5	3.43	745.8	2.5 ± 0.9

[a] data from Marchelli et al., [32] except for SY, LY, GY, and lactic acid yield.
[b] N not indicated as it was null in all cases, standard deviations all lower than 0.1%.

Table 3
Product yields and properties of the different phases from the HTC of PET.

HTC temp (°C)	Solid[b]				Liquid			Gas
	SY (%)	C (%)	H (%)	O (%)	LY (%)	TOC (g/L)	pH	GY (%)
Raw material	–	62.0	4.6	33.4	–	–	–	–
Raw PET[a]	–	62.5	4.2	33.3	–	–	–	–
Raw terephthalic acid[a]	–	57.9	3.6	38.5	–	–	–	–
180	98.7 ± 0.9	61.9	4.6	33.5	0.3 ± 0.9	1.9	5.38	0.9 ± 0.8
200	97.5 ± 1.5	61.2	4.7	34.1	1.7 ± 0.9	2.4	4.56	0.8 ± 0.7
220	81.6 ± 2.5	57.0	4.5	38.4	17.8 ± 2.8	7.8	4.75	0.6 ± 0.4
250	79.0 ± 1.6	56.4	3.9	39.6	19.6 ± 2.3	11.6 ± 0.5	4.78	1.4 ± 0.7

[a] from chemical formula.
[b] N and ash not indicated as they were null in all cases, standard deviations all lower than 0.7%.

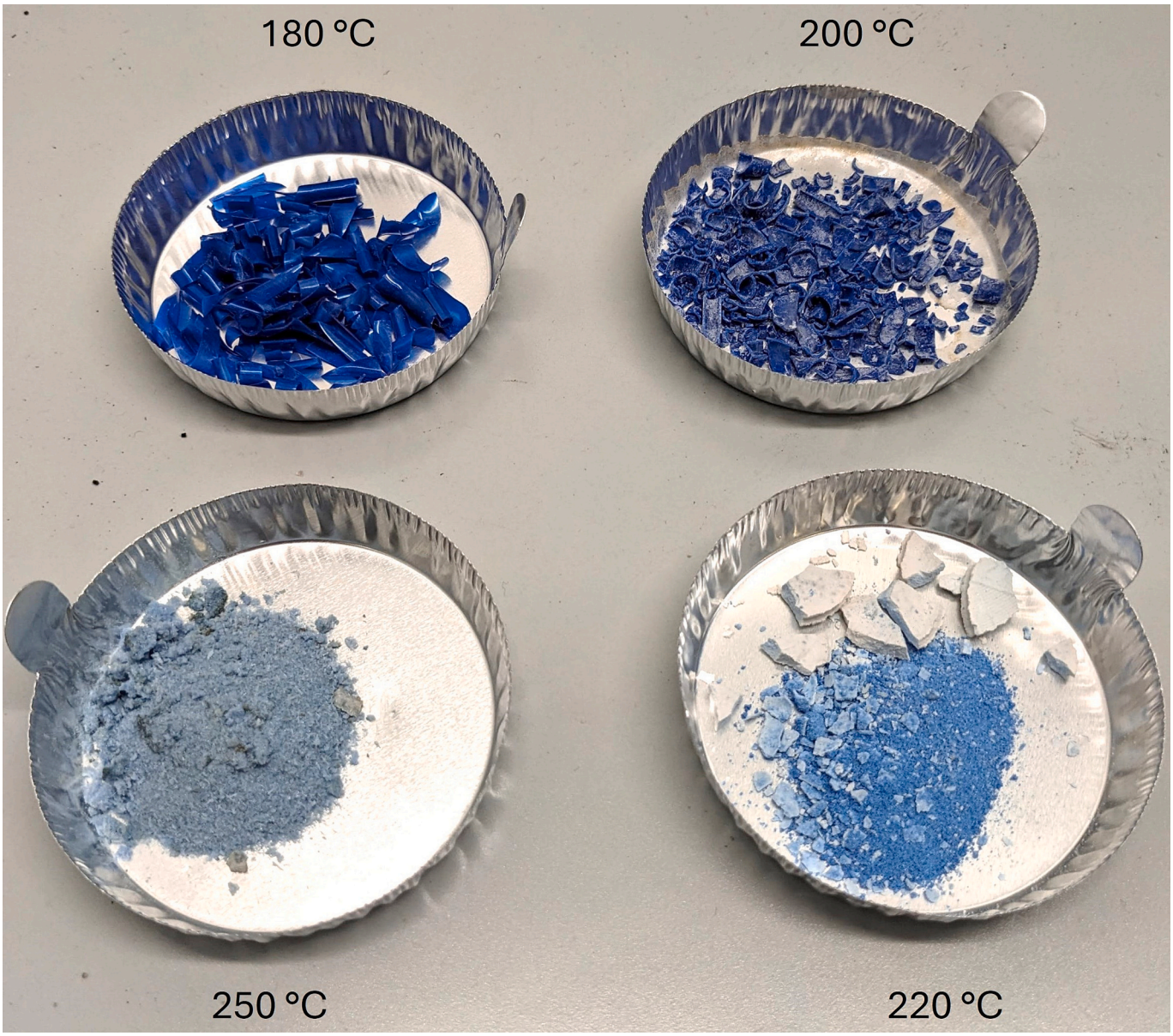

Fig. 5. The solids obtained from the HTC of PET at various temperatures.

The solid yields are close to 100% at lower temperatures, while they approach approximately 80% at higher temperatures. ^{1}H NMR analyses show that at 180 and 200 °C, the solid fraction is mainly constituted by unreacted PET (Figs. S25-S27). At 220 °C, signals concerning the PET hydrolysis products, such as bis-(2-hydroxyethyl) terephthalate, become prominent, underlying a more efficient polymeric degradation (Fig. S28). Interestingly, at 250 °C, a complete degradation occurs, yielding a solid fraction composed of 99% terephthalic acid (Fig. S29).

Indeed, a minor portion of the terephthalic acid is still dissolved in the liquid and therefore may not be accounted for in the solid fraction that we recover. This also means that, at 220 and 250 °C, the LY data reported in Table 3 (calculated by difference) are underestimated to a significant extent. Indeed, stoichiometrically, the full hydrolysis of 1 g of PET yields about 1.2 g of products (terephthalic acid and ethylene glycol). The advancement of the hydrolysis reaction is also confirmed by the properties of the liquid, which becomes richer in carbon and more acidic as the HTC temperature increases.

Fig. 6 shows the FTIR analysis of PET treated at different temperatures. Consistently with the results obtained for PBAT (BPBAGS), at high temperature, PET shows the development of broad signals in the -CH bending region (3120–2470 cm^{-1}) related to multiple new degradation species. The shifting of the carbonyl signals from 1720 to 1680 cm^{-1}, the appearance of -OH bending signals at 1420 cm^{-1} and 928 cm^{-1}, and the vanishing of the signals at 1340 cm^{-1} (the wagging vibrational modes of the ethylene glycol segment) and 1090 cm^{-1} testify the hydrolysis of the macromolecular structure, the formation of acid moieties, and the depletion of the ethylene glycol units [63].

Fig. 7 reports the product yields calculated by the ^{1}H NMR analysis of the liquid recovered from the HTC process. The main product is ethylene glycol, ranging from 2.6 mg/g_0 at 180 °C to 450.6 mg/g_0 at 250 °C (Figs. S13-S16). We also observed very low yields of terephthalic acid, and slightly higher yields of two of its compounds with ethylene glycol: mono(2-hydroxyethyl) terephthalate (MHET) and bis(2-hydroxyethyl) terephthalate (BHET). All these compounds are, however, not very soluble in water, which explains why their yields are relatively low and is in line with the high amounts of solids recovered.

3.4. HDPE, LDPE, PS, PP

This sub-section describes the behaviour of the four remaining plastics that we tested (HDPE, LDPE, PP, and PS). Their results are collated because of their similarity: as reported in Table 4, even at 250 °C, HTC is unable to degrade these plastics to any extent, and the mass of the recovered solid is virtually equivalent to the initial one. There is, however, a visible change in their appearance: after the process, they are found as a single piece at the top of the liquid phase, much more compact than the initial materials. As an example, Fig. 8 displays the block recovered after the HTC of PS. This well aligns with the fact that the melting temperatures of these polymers are all lower than

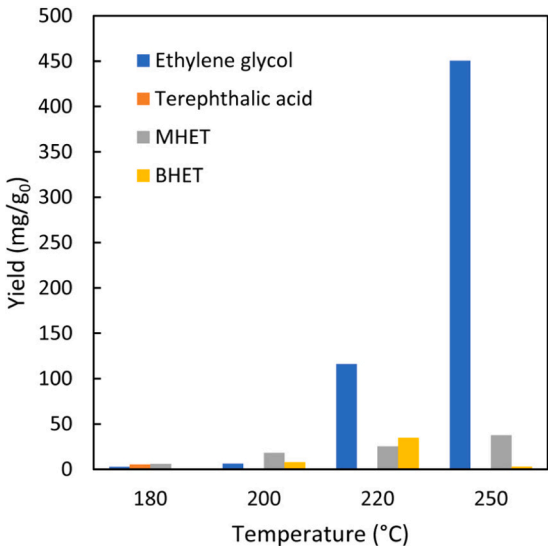

Fig. 7. Yields of products in the liquid phase from the HTC of PET. Refer to the nomenclature section for the acronyms.

250 °C. Therefore, while HTC is unable to cause any chemical modification to their structure, it may still be a good strategy to compact them, reducing the transport costs and facilitating their feeding to subsequent treatments.

Our findings are generally consistent with the literature described in the introduction, except for the work by Che et al. [64], who reported a 47.9% SY after the HTC of PS at 200 °C. To partially justify this discrepancy, we observe that since their PS was recovered from waste bins and has a non-null oxygen content, it is possible that it was not pure.

The liquids obtained from these materials were also subjected to NMR analyses. As expected, these did not detect any compound in significant concentrations, confirming that no hydrolysis occurs (Figs. S17-S20).

3.5. Mixture of bioplastics and plastics

The results from the HTC of the MIX are reported in Table 5. The most interesting output is that the process seems able to perform a rough

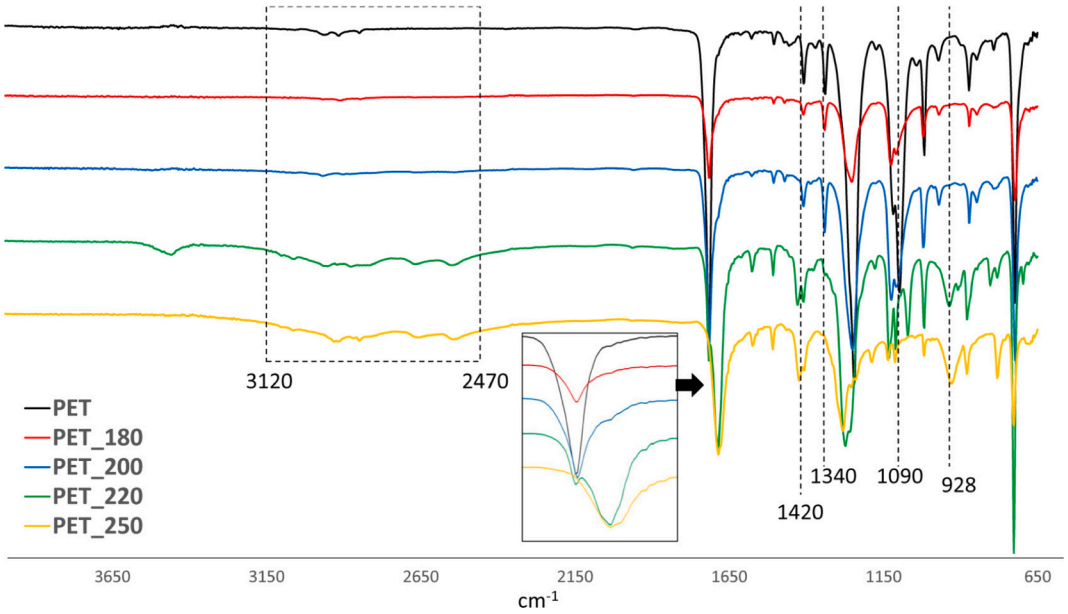

Fig. 6. FTIR spectra of the solids from the HTC of PET.

Table 4
Product yields and properties of the different phases from the HTC of HDPE, LDPE, PP, and PS.

Material	Conditions	Solid[a]			Liquid			Gas
		SY (%)	C (%)	H (%)	LY (%)	TOC (g/L)	pH	GY (%)
HDPE	Raw	–	86.6	13.3	–	–	–	–
	250 °C	99.3 ± 0.7	89.5	10.5	0.2 ± 1.0	1.2	6.38	0.5 ± 0.3
LDPE	Raw	–	86.2	13.7	–	–	–	–
	250 °C	100.0	86.5	13.5	0.0	3.5	5.97	0.0
PP	Raw	–	84.9	15.1	–	–	–	–
	250 °C	99.5 ± 0.5	85.8	14.1	0.5 ± 0.5	0.2	6.30	0.0
PS	Raw	–	93.7	6.3	–	–	–	–
	250 °C	99.5 ± 0.5	93.7	6.3	0.5 ± 0.5	0.4	5.90	0.0

[a] N, O and ash not indicated since they were null in all cases, standard deviations lower than 0.1% in all cases.

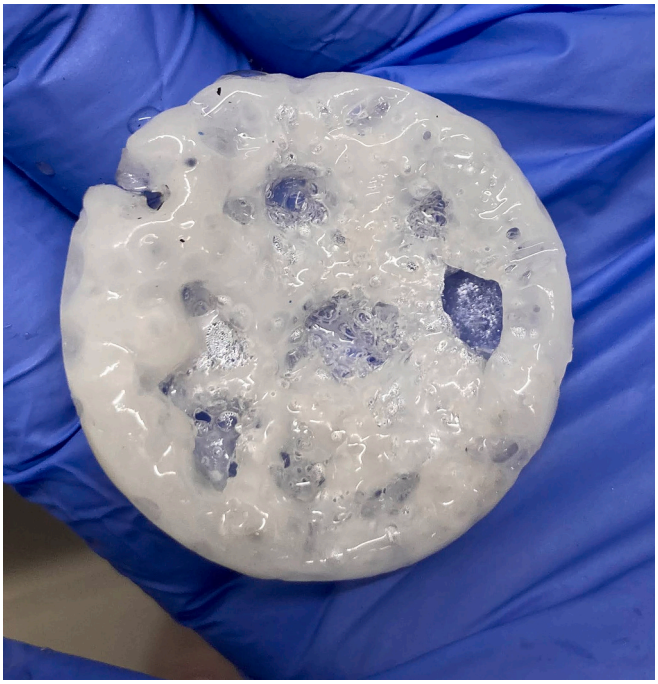

Fig. 8. PS after HTC at 250 °C (the appearance is very similar for all four plastics).

separation of bioplastics and plastics: while bioplastics are partially hydrolysed and their solid residue is found on the reactor's bottom and wall, the plastics behave in the same way as described in the previous sub-section, forming a compact block at the top of the reactor. PET shows an intermediate behaviour: it is found together with the other plastics at lower temperatures, and it disintegrated at higher temperatures. The coarse block of plastics is heterogeneous, with layers of different polymers still clearly distinguishable: as an example, Fig. 9 depicts the one that was recovered after the test at 220 °C, while pictures from the other tests can be found in the Supporting Information (Fig. S31-S34). Such a mixed product is unsuitable for mechanical recycling, but may be more appropriate for gasification or pyrolysis than the original waste mixture, owing to its higher bulk density and lower oxygen content (as all tested traditional plastics have a null oxygen content, except for PET).

The data suggest no evident synergistic or inhibitory effect on the products yields from processing the materials together: the experimental SYs closely match the weighted averages of the single-material SYs (indicated in Table 5 as "Theoretical SY"). The TOC and pH values confirm that higher HTC temperatures favour the dissolution of compounds in the liquid phase, with no evident benefits above 220 °C. For these experiments, the ultimate analysis of the solid products is not reported because the results were not reliable: even after milling, the material is not homogeneous, so it is impossible to feed the elemental analyser with samples that are truly representative of the whole block.

The NMR analyses of the liquid phase produced by the HTC of the MIX reveal a complex array of products, whose yields are displayed in Fig. 10 (Figs. S21-S24). The composition is mainly influenced by cPLA and BPBAGS, the two materials most affected by HTC. Lactic acid originates from both feedstocks and is by far the dominant compound. Even from this heterogeneous mixture, it reaches a concentration up to 25.9 g/L, an amount that is even higher than the theoretically expected value (reported in Table S2) and could justify targeted recovery. The behaviour of other compounds diverges from their expected trends as

Fig. 9. The solid block recovered after the HTC of the MIX at 220 °C.

Table 5
Product yields and properties of the different phases from the HTC of MIX.

HTC temp (°C)	Solid		Liquid			Gas
	SY (%)	Theoretical SY (%)	LY (%)	TOC (g/L)	pH	GY (%)
180	75.3 ± 0.8	74.7	23.9 ± 1.0	9.9 ± 0.4	3.60	0.8 ± 0.3
200	71.9 ± 0.6	73.3	27.7 ± 1.2	12.5 ± 0.5	3.60	0.9 ± 0.7
220	67.4 ± 0.8	67.0	31.8 ± 1.2	18.5	3.55	0.8 ± 0.3
250	65.1 ± 2.9	62.8	33.8 ± 3.2	21.0	3.32	1.1 ± 0.3

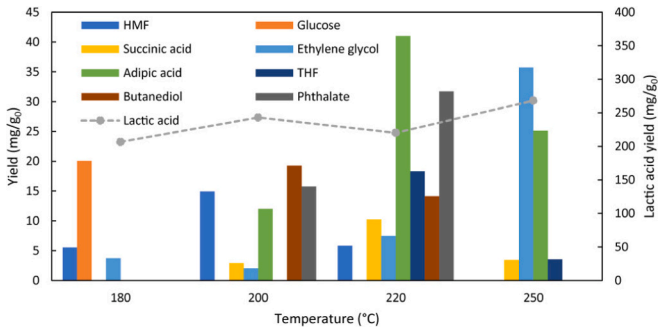

Fig. 10. Yields of products in the liquid phase from the HTC of the MIX. Refer to the nomenclature section for the acronyms.

well. The most notable case is that of starch amylose, which is a major compound in the decomposition of BPBAGS at 180 °C (Fig. S5) but is instead completely absent here (Fig. S21). Similarly, glucose is found at a lower concentration at 180 °C and is completely absent at 200 °C, while succinic and adipic acids and THF do not increase monotonously, reaching their maximum concentration at 220 °C. Phthalates also reach much higher concentrations than they theoretically should, meaning that their production or release is favoured. These observations imply that the different reaction environment, more acidic due to the abundance of lactic acid, affects the reaction pathways, favouring the formation of certain compounds over others. However, given that the solid yields are instead in line with their theoretical values, the synergies are likely only between cPLA and BPBAGS, causing a rearrangement of the dissolved products, but leaving the behaviour of traditional plastics remain unaffected.

In summary, the HTC of this polymer mixture appears as an interesting option to recover lactic acid, with the extreme temperatures of 180 and 250 °C producing the simplest mixtures, likely to facilitate its separation. At 180 °C, PET and some portions of the BPBAGS are not hydrolysed and remain in the recovered solid, while at 250 °C, both are mostly dissolved, and the recovered solid block consists nearly entirely of polyolefins and PS. Similarly to pure BPBAGS, if the liquid mixture is to be sent to anaerobic digestion, 180 °C appears as the best temperature as it results in only a few compounds, easily degradable by bacteria, except for HMF. A specific discussion on the possible detrimental effects of HMF and other compounds in anaerobic digestion is provided in the next sub-section.

3.6. Practical implications and future outlook

The potential separation of bioplastics and plastics is one of the most interesting aspects of applying the HTC process to mixed waste streams. In our experiments, plastics (except for PET at higher temperatures) appear to melt under the applied thermal conditions, consistent with their melting temperatures, and then solidify again upon cooling. Although ascertaining the behaviour of a pressurised device is difficult (and unfeasible with our current experimental capacity), it is likely that water and molten plastics form two distinct liquid phases, with the plastic phase floating above due to its lower density. This interpretation is supported by the consistent observation that, after cooling, a compacted plastic layer is found at the top of the reactor.

Nonetheless, our experiments were performed in a lab-scale, unstirred batch reactor, which does not reflect the industrial practise. Industrial HTC reactors are typically stirred and, in some cases, operated continuously. To facilitate phase separation and prevent plastic deposition on internal moving components, one possible strategy would be to perform the cooling step in a separate decanter unit. This approach is analogous to industrial processes involving immiscible liquid phases, such as the transesterification of fatty acids for biodiesel production [65]. The recovered plastic fraction could then be quantitatively extruded into pellets or other easily handled forms to enable downstream processing.

The energy requirements of the process should also be evaluated once its target mixture and scope have been defined. The energy demand of HTC is generally reported to be relatively modest (approximately 100 kWh_{heat}/t) with internal heat recovery within the process [66].

The presence of an array of chemical products may pose challenges if the liquid mixture is directed to anaerobic digestion. While certain compounds, such as lactic acid, are very well tolerated by anaerobic bacteria and are converted to biogas almost entirely [67], other compounds are known to potentially inhibit their activity. Table 6 summarises their effects in anaerobic digestion, the maximum concentrations detected in the present experimental campaign, and the maximum acceptable concentrations reported in the literature.

It should be noted that the liquid phase obtained from the HTC of mixed bioplastics and plastics is unlikely to be treated by anaerobic digestion as a standalone stream. In practical scenarios, this liquid fraction would represent only a small portion of the overall material processed and would likely be co-treated with other substrates. Consequently, the concentrations of the abovementioned inhibitory compounds will be at least one order of magnitude lower that those measured in this study, which in most cases would be sufficient to fall below problematic thresholds. Nonetheless, the maximum concentrations of these compounds are all detected at 200–250 °C and they are lower in the tests performed at 180 °C and in those on MIX. This observation further supports the well-established conclusion that 180 °C is the most suitable temperature for HTC when used as a pre-treatment prior to anaerobic digestion.

Table 6
Effects of some compounds in anaerobic digestion.

Compound	Effect in anaerobic digestion	Maximum concentration in the present campaign	Maximum acceptable concentration in anaerobic digestion
5-HMF	Interferes with cell growth, suppresses glycolysis enzymes, damages DNA [68].	5.8 g/L (from BPBAGS at 200 °C)	Well tolerated below 0.4 g/L, while complete inhibition of methanogenesis is seen above 2 g/L [68].
THF	Inhibits enzymes and can disrupt the metabolism of microorganisms [69].	4.9 g/L (from BPBAGS at 250 °C)	At 1.5 g/L biodegradation starts being hindered [70].
Ethylene glycol	Well tolerated and degraded by anaerobic bacteria, but at high concentrations may cause pH inhibition due to the accumulation of volatile acids [71].	44.2 g/L (from PET at 250 °C)	Starts causing problems above 10 g/L.
Phthalates	Classified as priority pollutants with associated carcinogenic, mutagenic and teratogenic effects. Short-chain phthalates are easily biodegradable, but long-chain phthalates tend to accumulate and negatively affect biogas production [72].	3.1 g/L (from MIX at 220 °C)	Depends on the type of phthalate, but above 0.06–0.10 g/L negative effects start being observed [73].

4. Conclusions

This study confirms the effectiveness of HTC in the treatment of bioplastics. Crystallised PLA undergoes complete hydrolysis to lactic acid starting from 180 °C, with no significant formation of by-products even at higher temperatures. Regarding Mater-Mater-Bi® constituents, starch hydrolyses at 180 °C, producing amylose, which is further converted into glucose and related compounds, especially as the temperature increases. In contrast, PBAT shows greater thermal stability, initiating hydrolysis only above 200 °C and yielding mainly succinic acid, and butanediol. Both tested bioplastic items (crystallised PLA spoons and compostable Mater-Bi® bags) were fully disintegrated at 180 °C, suggesting that HTC can mitigate the mechanical and hydraulic issues these materials pose to anaerobic digesters, regardless of the biogas yields from the HTC products, which will be tested in future works. Among conventional plastics, only PET undergoes significant transformation under HTC, fully hydrolysing into ethylene glycol and terephthalic acid at 250 °C. The latter can be qualitatively recovered in solid form, opening opportunities for recovery and recycling of this important building block. In contrast, HDPE, LDPE, PS, and PP remain chemically unchanged, though they tend to fuse into a compact solid mass that floats on the liquid phase.

Treating bioplastics and plastics in a mixture reveals no major synergistic effects: the observed behaviour in terms of products yields is mostly a superposition of the behaviour of the single items, while the liquid phase composition slightly changes, likely due to the more acidic environment.

Co-HTC of bioplastics and plastics shows however a noteworthy practical potential, as it enables a physical separation between bioplastics and traditional plastics. Bioplastics are indeed disintegrated and hydrolysed, and are found in the liquid phase and on the reactor walls, while plastics (except for PET at 220–250 °C) coalesce in a compact block that is found at the top of the liquid phase. While a scale-up to an industrial-scale stirred reactor would introduce further challenges, the underlying principles are expected to hold, offering a pathway to direct each material class toward the most suitable downstream process.

Some aspects require further investigation. Although no toxic by-products were identified via NMR, the formation of trace inhibitory compounds cannot be ruled out and may impact microbial activity. Moreover, it is likely that the mixtures to be treated in real-life scenarios also contain organic residues. Future work will thus deal with the behaviour of more realistic waste mixtures, assessing how the liquid obtained from HTC responds to anaerobic digestion.

Nomenclature

BHET	bis(2-hydroxyethyl) terephthalate
FTIR	Fourier-transform infrared spectroscopy
GY	gas yield
HDPE	high-density polyethylene
HMF	5-hydroxymethylfurfural
HTC	hydrothermal carbonization
LDPE	low-density polyethylene
LY	liquid yield
MHET	monohydroxyethyl terephthalate
NMR	nuclear magnetic resonance
OFMSW	organic fraction of municipal solid waste
PBAT	poly(butylene adipate terephthalate)
PET	poly(ethylene terephthalate)
PLA	poly(lactic acid)
PP	polypropylene
PS	polystyrene
PVC	poly(vinyl chloride)
SY	solid yield
THF	tetrahydrofuran
TOC	total organic carbon

CRediT authorship contribution statement

Filippo Marchelli: Writing – original draft, Visualization, Validation, Software, Project administration, Methodology, Investigation, Formal analysis, Data curation, Conceptualization. **Claudio Gioia:** Writing – original draft, Validation, Resources, Methodology, Investigation, Formal analysis, Data curation, Conceptualization. **Sara Lombini:** Writing – original draft, Software, Investigation, Data curation. **Gianni Andreottola:** Writing – review & editing, Supervision, Resources, Project administration, Funding acquisition, Conceptualization. **Luca Fiori:** Writing – review & editing, Supervision, Resources, Project administration, Funding acquisition, Conceptualization.

Declaration of competing interest

The authors declare the following financial interests/personal relationships which may be considered as potential competing interests: Filippo Marchelli reports financial support was provided by European Union. If there are other authors, they declare that they have no known competing financial interests or personal relationships that could have appeared to influence the work reported in this paper.

Acknowledgements

The publication was created with the co-financing of the European Union–FSE-REACT-EU, PON Research and Innovation 2014-2020 DM1062/2021.

Appendix A. Supplementary data

Supplementary data to this article can be found online at https://doi.org/10.1016/j.cej.2026.174526.

Data availability

Data will be made available on request.

References

[1] S. Chen, Y.H. Hu, Advancements and future directions in waste plastics recycling: from mechanical methods to innovative chemical processes, Chem. Eng. J. 493 (2024) 152727, https://doi.org/10.1016/J.CEJ.2024.152727.
[2] Plastics Europe, Plastics – The Fast Facts 2023 • Plastics Europe, (n.d.). https://plasticseurope.org/knowledge-hub/plastics-the-fast-facts-2023/ (accessed March 12, 2025).
[3] P. Sambyal, P. Najmi, D. Sharma, E. Khoshbakhti, H. Hosseini, A.S. Milani, M. Arjmand, Plastic recycling: challenges and opportunities, Can. J. Chem. Eng. (2024), https://doi.org/10.1002/CJCE.25531.
[4] Z.O.G. Schyns, M.P. Shaver, Z.O.G. Schyns, M.P. Shaver, Mechanical recycling of packaging plastics: a review, Macromol. Rapid Commun. 42 (2021) 2000415, https://doi.org/10.1002/MARC.202000415.
[5] European Bioplastics e.V, BIOPLASTICS MARKET DEVELOPMENT UPDATE 2023. https://www.european-bioplastics.org/bioplastics-market-development-update-2023-2/, 2024. (Accessed 19 July 2024).
[6] F. Battista, N. Frison, D. Bolzonella, Can bioplastics be treated in conventional anaerobic digesters for food waste treatment? Environ. Technol. Innov. 22 (2021) 101393 https://doi.org/10.1016/J.ETI.2021.101393.
[7] G. Dolci, L. Rigamonti, M. Grosso, The challenges of bioplastics in waste management, Waste Manag. Res. 41 (2023) 1281–1282, https://doi.org/10.1177/0734242X231181999.
[8] F. Marchelli, L. Fiori, The growing problem of waste bioplastics disposal, and a way to tackle it, Waste Manag. 201 (2025) 114786, https://doi.org/10.1016/J.WASMAN.2025.114786.
[9] E. Ansink, L. Wijk, F. Zuidmeer, No clue about bioplastics, Ecol. Econ. 191 (2022) 107245, https://doi.org/10.1016/j.ecolecon.2021.107245.
[10] N. Mhaddolkar, T.F. Astrup, A. Tischberger-Aldrian, R. Pomberger, D. Vollprecht, Challenges and opportunities in managing biodegradable plastic waste: a review, Waste Manag. Res. (2024), https://doi.org/10.1177/0734242X241279902.
[11] N. Mhaddolkar, C. Lodato, A. Tischberger-Aldrian, D. Vollprecht, T. Fruergaard Astrup, Biodegradable plastics – where to throw? A life cycle assessment of waste collection and management pathways in Austria, Waste Manag. 190 (2024) 578–592, https://doi.org/10.1016/j.wasman.2024.10.018.
[12] L. Dilkes-Hoffman, P. Ashworth, B. Laycock, S. Pratt, P. Lant, Public attitudes towards bioplastics – knowledge, perception and end-of-life management, Resour.

Conserv. Recycl. 151 (2019) 104479, https://doi.org/10.1016/j.resconrec.2019.104479.
[13] J. Cristóbal, P. Federica Albizzati, M. Giavini, D. Caro, S. Manfredi, D. Tonini, Management practices for compostable plastic packaging waste: impacts, challenges and recommendations, Waste Manag. 170 (2023) 166–176, https://doi.org/10.1016/j.wasman.2023.08.010.
[14] M.J. Staplevan, A.J. Ansari, A. Ahmed, F.I. Hai, Impact of bioplastic contamination on the mechanical recycling of conventional plastics, Waste Manag. 185 (2024) 1–9, https://doi.org/10.1016/j.wasman.2024.05.028.
[15] M.S. Qureshi, A. Oasmaa, H. Pihkola, I. Deviatkin, A. Tenhunen, J. Mannila, H. Minkkinen, M. Pohjakallio, J. Laine-Ylijoki, Pyrolysis of plastic waste: opportunities and challenges, J. Anal. Appl. Pyrolysis 152 (2020) 104804, https://doi.org/10.1016/j.jaap.2020.104804.
[16] C. Moliner, G. Pasquale, E. Arato, Municipal plastic waste recycling through Pyrogasification, Energies 17 (2024) 1206, https://doi.org/10.3390/en17051206.
[17] R. Darzi, Y. Dubowski, J.L. Goldfarb, M. Karod, D. Sills, R. Posmanik, Hydrothermal processing of multilayer plastic film for cascaded valorization of nonrecyclable waste, ACS Sustain. Chem. Eng. (2023), https://doi.org/10.1021/ACSSUSCHEMENG.3C06003.
[18] J. Colwell, S. Pratt, P. Lant, B. Laycock, Hazardous state lifetimes of biodegradable plastics in natural environments, Sci. Total Environ. 894 (2023) 165025, https://doi.org/10.1016/j.scitotenv.2023.165025.
[19] S.V. Afshar, A. Boldrin, T.F. Astrup, A.E. Daugaard, N.B. Hartmann, Degradation of biodegradable plastics in waste management systems and the open environment: a critical review, J. Clean. Prod. 434 (2024) 140000, https://doi.org/10.1016/j.jclepro.2023.140000.
[20] M.E. Iñiguez, J.A. Conesa, A. Fullana, Marine debris occurrence and treatment: a review, Renew. Sust. Energ. Rev. 64 (2016) 394–402, https://doi.org/10.1016/j.rser.2016.06.031.
[21] Y. Luo, D. Zhang, J. Cheng, G. Liang, G. Ren, J. Xu, H. Tang, S. Cao, Au@MoS boosted carbon nitride for selective photoreforming of plastic waster: synergistic hydrogen production and value-added chemicals generation, Adv. Powder Mater. 5 (2026) 100366, https://doi.org/10.1016/j.apmate.2025.100366.
[22] K.Y. Tang, C.Y. Chan, C.H.T. Chai, B.Q.L. Low, Z.Y. Toh, B.W.L. Wong, J.Z.X. Heng, Z. Li, C.-L.K. Lee, X.J. Loh, C.-H. Wang, E. Ye, Thermochemical valorization of waste plastic for production of synthetic fuels, fine chemicals, and carbon nanotubes, ACS Sustain. Chem. Eng. 12 (2024) 1769–1796, https://doi.org/10.1021/acssuschemeng.3c06276.
[23] I. Ayuso-Díaz, S. Perez-Gil, G. Lopez, L. Santamaria, F.J. Antoñanzas-González, Progress on waste plastics gasification process: a review of operating conditions, reactors and catalysts for clean syngas production and tar abatement, Int. J. Hydrog. Energy 148 (2025) 150000, https://doi.org/10.1016/j.ijhydene.2025.06.190.
[24] R.P. Ipiales, M.A. de la Rubia, E. Diaz, A.F. Mohedano, J.J. Rodriguez, Integration of hydrothermal carbonization and anaerobic digestion for energy recovery of biomass waste: an overview, Energy Fuel 35 (2021) 17032–17050, https://doi.org/10.1021/acs.energyfuels.1c01681.
[25] M. Ahmed, G. Andreottola, S. Elagroudy, M.S. Negm, L. Fiori, Coupling hydrothermal carbonization and anaerobic digestion for sewage digestate management: influence of hydrothermal treatment time on dewaterability and biomethane production, J. Environ. Manag. 281 (2021) 111910, https://doi.org/10.1016/j.jenvman.2020.111910.
[26] M. Wilk, M. Śliz, K. Czerwińska, M. Gajek, I. Kalemba-Rec, Improvements in dewaterability and fuel properties of hydrochars derived from hydrothermal co-carbonization of sewage sludge and organic waste, Renew. Energy 227 (2024) 120547, https://doi.org/10.1016/j.renene.2024.120547.
[27] L. Mu, L. Zhang, J. Ma, K. Zhu, C. Chen, A. Li, Enhanced biomethanization of waste polylactic acid plastic by mild hydrothermal pretreatment: Taguchi orthogonal optimization and kinetics modeling, Waste Manag. 126 (2021) 585–596, https://doi.org/10.1016/j.wasman.2021.03.044.
[28] S. Im, I. Hwang, K. Weonjae, D.-H. Kim, J.-H. Kang, S. Kang, Enhancing methane production potential of biodegradable plastics by hydrothermal pretreatment, Environ. Technol. Innov. 34 (2024) 103599, https://doi.org/10.1016/j.eti.2024.103599.
[29] G. Cazaudehore, R. Guyoneaud, C. Vasmara, P. Greuet, E. Gastaldi, R. Marchetti, F. Leonardi, R. Turon, F. Monlau, Impact of mechanical and thermo-chemical pretreatments to enhance anaerobic digestion of poly(lactic acid), Chemosphere 297 (2022) 133986, https://doi.org/10.1016/j.chemosphere.2022.133986.
[30] C. Vasmara, G. Cazaudehore, E. Ceotto, R. Marchetti, C. Sambusiti, F. Monlau, Alkali, thermal, or thermo-alkali pre-treatment to improve the anaerobic digestion of poly(lactic acid)? Water Res. 258 (2024) 121744 https://doi.org/10.1016/j.watres.2024.121744.
[31] X. Wang, Y. Sun, M. Liu, G. You, T. Fan, H. Wu, L. Xu, X. Zhao, D. Ma, Hydrothermal processing of polylactic acid: analysis of intermediate products and toxicity evaluation of anaerobically digestated residues, Chem. Eng. J. 502 (2024) 157634, https://doi.org/10.1016/J.CEJ.2024.157634.
[32] F. Marchelli, M. Mattonai, R. Ferrentino, J. La Nasa, N. Pecorelli, F. Modugno, G. Andreottola, E. Ribechini, L. Fiori, Fostering bioplastics circularity through hydrothermal treatments: degradation behavior and products, ACS Sustain. Chem. Eng. 12 (2024) 9257–9267, https://doi.org/10.1021/acssuschemeng.4c02174.
[33] G. Dolci, A. Catenacci, F. Malpei, M. Grosso, Effect of paper vs. bioplastic bags on food waste collection and processing, Waste Biomass Valor. 12 (2021) 6293–6307, https://doi.org/10.1007/s12649-021-01448-4.
[34] R. Yang, K. Jan, C. Chen, W. Chen, K.C.-W. Wu, Thermochemical conversion of plastic waste into fuels, chemicals, and value-added materials: a critical review and outlooks, ChemSusChem 15 (2022), https://doi.org/10.1002/cssc.202200171.
[35] Y. Shen, A review on hydrothermal carbonization of biomass and plastic wastes to energy products, Biomass Bioenergy 134 (2020) 105479, https://doi.org/10.1016/j.biombioe.2020.105479.
[36] G. Farru, J.A. Libra, K.S. Ro, C. Cannas, C. Cara, A. Muntoni, M. Piredda, G. Cappai, Valorization of face masks produced during COVID-19 pandemic through hydrothermal carbonization (HTC): a preliminary study, Sustainability 15 (2023) 9382, https://doi.org/10.3390/su15129382.
[37] M.E. Iñiguez, J.A. Conesa, A. Fullana, Hydrothermal carbonization (HTC) of marine plastic debris, Fuel 257 (2019) 116033, https://doi.org/10.1016/j.fuel.2019.116033.
[38] Y. Lin, X. Ma, X. Peng, Z. Yu, Hydrothermal carbonization of typical components of municipal solid waste for deriving hydrochars and their combustion behavior, Bioresour. Technol. 243 (2017) 539–547, https://doi.org/10.1016/j.biortech.2017.06.117.
[39] X. Zhao, L. Zhan, B. Xie, B. Gao, Products derived from waste plastics (PC, HIPS, ABS, PP and PA6) via hydrothermal treatment: characterization and potential applications, Chemosphere 207 (2018) 742–752, https://doi.org/10.1016/j.chemosphere.2018.05.156.
[40] N. Kaewtrakulchai, S. Chanpee, S. Jadsadajerm, S. Wongrerkdee, K. Manatura, A. Eiad-Ua, Co-hydrothermal carbonization of polystyrene waste and maize Stover combined with KOH activation to develop nanoporous carbon as catalyst support for catalytic hydrotreating of palm oil, Carbon Resour. Convers. 7 (2024) 100231, https://doi.org/10.1016/j.crcon.2024.100231.
[41] B.R. de A. Moreira, V.H. Cruz, M.R. Barbosa Júnior, M.D. Meneses, P.R.M. Lopes, R. P. da Silva, Agro-residual biomass and disposable protective face mask: a merger for converting waste to plastic-fiber fuel via an integrative carbonization-pelletization framework, Biomass Convers. Biorefinery (2022), https://doi.org/10.1007/s13399-022-03285-4.
[42] M.T. Islam, M.T. Reza, Evaluation of fuel and combustion properties of hydrochar derived from co-hydrothermal carbonization of biomass and plastic, Biomass Bioenergy 172 (2023) 106750, https://doi.org/10.1016/j.biombioe.2023.106750.
[43] M. Farghali, A. Shimahata, I.M.A. Mohamed, M. Iwasaki, J. Lu, I. Ihara, K. Umetsu, Integrating anaerobic digestion with hydrothermal pretreatment for bioenergy production: waste valorization of plastic containing food waste and rice husk, Biochem. Eng. J. 186 (2022) 108546, https://doi.org/10.1016/j.bej.2022.108546.
[44] H. Abedsoltan, A focused review on recycling and hydrolysis techniques of polyethylene terephthalate, Polym. Eng. Sci. 63 (2023) 2651–2674, https://doi.org/10.1002/pen.26406.
[45] C.N. Onwucha, C.O. Ehi-Eromosele, S.O. Ajayi, M. Schaefer, S. Indris, H. Ehrenberg, Uncatalyzed neutral hydrolysis of waste PET bottles into pure terephthalic acid, Ind. Eng. Chem. Res. (2023), https://doi.org/10.1021/ACS.IECR.2C04117.
[46] W. Yang, R. Liu, C. Li, Y. Song, C. Hu, Hydrolysis of waste polyethylene terephthalate catalyzed by easily recyclable terephthalic acid, Waste Manag. 135 (2021) 267–274, https://doi.org/10.1016/j.wasman.2021.09.009.
[47] J. Poerschmann, B. Weiner, S. Woszidlo, R. Koehler, F.-D. Kopinke, Hydrothermal carbonization of poly(vinyl chloride), Chemosphere 119 (2015) 682–689, https://doi.org/10.1016/j.chemosphere.2014.07.058.
[48] Y. Shen, S. Yu, S. Ge, X. Chen, X. Ge, M. Chen, Hydrothermal carbonization of medical wastes and lignocellulosic biomass for solid fuel production from lab-scale to pilot-scale, Energy 118 (2017) 312–323, https://doi.org/10.1016/j.energy.2016.12.047.
[49] Y. Yu, B. Zhu, Y. Ding, P. Li, S. Ge, Hydrothermal carbonization of food waste digestates and polyvinyl chloride: focus on dechlorination performance and fuel characteristics, Biomass Convers. Biorefinery 13 (2023) 16161–16168, https://doi.org/10.1007/s13399-022-02957-5.
[50] Q. Liu, G. Ji, X. Li, G. Zhang, X. Zhang, X. Zhang, L. Han, Insights into PVC-promoted hydrothermal carbonization of manure: Dechlorination, inorganic metals removal, and combustion behaviors, Chem. Eng. J. 491 (2024) 152167, https://doi.org/10.1016/j.cej.2024.152167.
[51] N. Huang, P. Zhao, S. Ghosh, A. Fedyukhin, Co-hydrothermal carbonization of polyvinyl chloride and moist biomass to remove chlorine and inorganics for clean fuel production, Appl. Energy 240 (2019) 882–892, https://doi.org/10.1016/j.apenergy.2019.02.050.
[52] J. Zhang, Y. Chen, X. Xia, B. Fu, C. Lin, G. Jia, X. Cui, F. Liu, P. Zhao, Y. Li, Co-hydrothermal carbonization of polyvinyl chloride and lignocellulose biomasses for chlorine and inorganics removal, Waste Manag. 156 (2023) 198–207, https://doi.org/10.1016/j.wasman.2022.11.039.
[53] Y. Xue, L. Bai, M. Chi, X. Xu, L. Tai, Z. Chen, K. Yu, Z. Liu, Co-hydrothermal carbonization of lignocellulose biomass and polyvinyl chloride: the migration and transformation of chlorine, Chem. Eng. J. 446 (2022) 137155, https://doi.org/10.1016/j.cej.2022.137155.
[54] Market – European Bioplastics e.V., (n.d.). https://www.european-bioplastics.org/market/ (accessed August 27, 2024).
[55] L. Fiori, D. Basso, D. Castello, M. Baratieri, Hydrothermal carbonization of biomass: design of a batch reactor and preliminary experimental results, Chem. Eng. Trans. 37 (2014) 55–60, https://doi.org/10.3303/CET1437010.
[56] M.G. Zaman, H. Xu, Z. Bi, B. Patel, N. Samec, M. Vujanovic, Y. Guo, Biofuel production boosted by plastic waste: co-hydrothermal liquefaction of plastic and biomass toward sustainable energy, Ind. Eng. Chem. Res. 64 (2025) 1876–1893, https://doi.org/10.1021/acs.iecr.4c03663.
[57] P. Burguete, A. Corma, M. Hitzl, R. Modrego, E. Ponce, M. Renz, Fuel and chemicals from wet lignocellulosic biomass waste streams by hydrothermal carbonization, Green Chem. 18 (2016) 1051–1060, https://doi.org/10.1039/C5GC02296G.

[58] G. Ischia, M. Cutillo, G. Guella, N. Bazzanella, M. Cazzanelli, M. Orlandi, A. Miotello, L. Fiori, Hydrothermal carbonization of glucose: secondary char properties, reaction pathways, and kinetics, Chem. Eng. J. 449 (2022) 137827, https://doi.org/10.1016/j.cej.2022.137827.
[59] G. Ischia, F. Marchelli, N. Bazzanella, R. Ceccato, M. Calvi, G. Guella, C. Gioia, L. Fiori, Cellulose acetates in hydrothermal carbonization: a green pathway to valorize residual bioplastics, ChemSusChem 18 (2025), https://doi.org/10.1002/cssc.202401163.
[60] K. Elfehri Borchani, C. Carrot, M. Jaziri, Biocomposites of alfa fibers dispersed in the mater-Bi® type bioplastic: morphology, mechanical and thermal properties, Compos. Part A Appl. Sci. Manuf. 78 (2015) 371–379, https://doi.org/10.1016/J.COMPOSITESA.2015.08.023.
[61] J. Jian, Z. Xiangbin, H. Xianbo, An overview on synthesis, properties and applications of poly(butylene-adipate-co-terephthalate)–PBAT, Adv. Ind. Eng. Polym. Res. 3 (2020) 19–26, https://doi.org/10.1016/j.aiepr.2020.01.001.
[62] T.A.H. Nguyen, T.H. Bui, W.S. Guo, H.H. Ngo, Valorization of the aqueous phase from hydrothermal carbonization of different feedstocks: challenges and perspectives, Chem. Eng. J. 472 (2023) 144802, https://doi.org/10.1016/j.cej.2023.144802.
[63] Z. Chen, J.N. Hay, M.J. Jenkins, The thermal analysis of poly(ethylene terephthalate) by FTIR spectroscopy, Thermochim. Acta 552 (2013) 123–130, https://doi.org/10.1016/j.tca.2012.11.002.
[64] C.A. Che, K.M. Van Geem, P.M. Heynderickx, Enhancing sustainable waste management: hydrothermal carbonization of polyethylene terephthalate and polystyrene plastics for energy recovery, Sci. Total Environ. 946 (2024) 174110, https://doi.org/10.1016/j.scitotenv.2024.174110.
[65] Y.H. Shen, J.K. Cheng, J.D. Ward, C.C. Yu, Design and control of biodiesel production processes with phase split and recycle in the reactor system, J. Taiwan Inst. Chem. Eng. 42 (2011) 741–750, https://doi.org/10.1016/j.jtice.2011.01.010.
[66] R. Ferrentino, M. Langone, L. Fiori, G. Andreottola, Full-scale sewage sludge reduction technologies: a review with a focus on energy consumption, Water 15 (2023) 615, https://doi.org/10.3390/w15040615.
[67] R. Ferrentino, F. Marchelli, A. Bevilacqua, L. Fiori, G. Andreottola, Hydrothermal pre-treatments can make PLA and PBS bioplastics suitable for anaerobic digestion, J. Environ. Chem. Eng. 13 (2025) 116204, https://doi.org/10.1016/j.jece.2025.116204.
[68] Z. Tan, X. Li, C. Yang, H. Liu, J.J. Cheng, Inhibition and disinhibition of 5-hydroxymethylfurfural in anaerobic fermentation: a review, Chem. Eng. J. 424 (2021) 130560, https://doi.org/10.1016/j.cej.2021.130560.
[69] Y. Wang, L. Xu, H. Mei, L. Xuan, B. Zhang, J. Geng, M. Zheng, F. Dong, Enhanced anaerobic treatment of polybutadiene adipate terephthalate wastewater in up-flow anaerobic sludge blanket by pre-acidification: pollutants degradation and microbial succession, Desalin. Water Treat. 323 (2025) 101277, https://doi.org/10.1016/j.dwt.2025.101277.
[70] C.-H. Ni, C.-Y. Chang, Y.-C. Lin, J.C.-T. Lin, Simultaneous biodegradation of tetrahydrofuran, 3-buten-1-ol and 1,4-butanediol in real wastewater by a pilot high-rate UASB reactor, Int. Biodeterior. Biodegradation 143 (2019) 104698, https://doi.org/10.1016/j.ibiod.2019.05.015.
[71] J.M. Stewart, S.K. Bhattacharya, R.L. Madura, S.H. Mason, J.C. Schonberg, Anaerobic treatability of selected organic toxicants in petrochemical wastes, Water Res. 29 (1995) 2730–2738, https://doi.org/10.1016/0043-1354(95)00138-B.
[72] P. Wang, Y. Su, D. Wu, B. Xie, Plasticizers inhibit food waste anaerobic digestion performance by affecting microbial succession and metabolism, J. Hazard. Mater. 473 (2024) 134554, https://doi.org/10.1016/j.jhazmat.2024.134554.
[73] H.N. Gavala, F. Alatriste-Mondragon, R. Iranpour, B.K. Ahring, Biodegradation of phthalate esters during the mesophilic anaerobic digestion of sludge, Chemosphere 52 (2003) 673–682, https://doi.org/10.1016/S0045-6535(03)00126-7.